



HAL
open science

Automatic control strategy for catching a fixed-wing drone using a ground vehicle

A. Alatorre, Pedro Castillo Garcia, Rogelio Lozano

► **To cite this version:**

A. Alatorre, Pedro Castillo Garcia, Rogelio Lozano. Automatic control strategy for catching a fixed-wing drone using a ground vehicle. 26th IEEE International Conference on Intelligent Transportation Systems (ITSC 2023), Sep 2023, Bilbao, Spain, Spain. hal-04342801

HAL Id: hal-04342801

<https://hal.science/hal-04342801>

Submitted on 13 Dec 2023

HAL is a multi-disciplinary open access archive for the deposit and dissemination of scientific research documents, whether they are published or not. The documents may come from teaching and research institutions in France or abroad, or from public or private research centers.

L'archive ouverte pluridisciplinaire **HAL**, est destinée au dépôt et à la diffusion de documents scientifiques de niveau recherche, publiés ou non, émanant des établissements d'enseignement et de recherche français ou étrangers, des laboratoires publics ou privés.

Automatic control strategy for catching a fixed-wing drone using a ground vehicle

Armando Alatorre^{1,2}, Pedro Castillo¹ & Rogelio Lozano^{1,2}.

Abstract—This paper presents a control strategy designed in 3D for landing a fixed-wing drone on a moving ground vehicle. The control strategy focuses on leading the fixed-wing vehicle towards a desired trajectory while the control algorithms for the ground vehicle regulate its speed and tracks the relative position of the aerial vehicle in the $x - y$ plane. The desired trajectory for the aerial vehicle is based on a hyperbolic tangent function to perform a soft descending reaching the ground vehicle's altitude. The strategy allows the rendezvous of both vehicles obtaining a safe landing for the airplane. The methodology to determine the control laws is based on the Lyapunov analysis, guaranteeing the stability on each control stage. The strategy is evaluated in numerical simulations for validating the systems performance in closed loop.

I. INTRODUCTION

The growing development of new technologies has encouraged the study of Unmanned Aerial Vehicles (UAVs) thanks their capabilities to perform missions such as monitoring high-risk areas [1], target identification [2], tracking of a moving ground vehicle [3], and agriculture activities.

The research community has been working to innovate and improve autonomous navigation in different types of environments and conditions. The field of automatic control has a high impact on the development of novel applications, maneuvers, and theoretical validation of control algorithms. Diverse research projects have focused on missions of path planning [4], guidance strategies [5], cooperative control [6], payload transportation, and obstacle avoidance.

UAVs are commonly classified into multicopter and fixed-wing vehicles. Multicopter configuration is composed of two or more rotors. It can fly at hover, allowing high-precision maneuvers to be performed such as the manipulation of objects, and the exploration of high-risk areas. Otherwise, fixed-wing vehicles are suitable for missions of high altitudes, long distances, and high speeds [7]. The main advantage is the energy consumption [8], since its aerodynamic properties allow the generation of lift to maintain the flight.

Focusing our research on fixed-wing vehicles, one critical flight stage is the landing. Since, the aircraft must perform the maneuver with precision, guiding the aircraft to the desired target and avoiding wind disturbances, which are the main causes of accidents. Thus, this increases the motivation of the researcher community to perform a safe landing by applying the control theory.

For improving safe landing, some sensors, and embedded devices have been included in the aerial vehicle. These sensors allow the measurement of variables to improve the control algorithms such as the Global Position System (GPS) [9], and the Inertial Measurement Unit (IMU). In addition, some perception solutions are also included and they are based on computational vision algorithms, identify markers to align the drone towards a runway [10] or estimate its position and speed with respect to a target [11].

In the literature, it is possible to find the flight stages for landing a fixed-wing drone on a runway. For example in [12], the authors divided the landing process into three stages: a descending flight, flare maneuver, and taxiing. The conditions required to carry out a landing on a runway or flat zone are very strict to reduce the likelihood of accidents in the landing process.

Considering the previously, some fixed-wing drones perform missions in order to navigate during a lot of hours or transport payload. Therefore, they need to reduce their weight and delete the landing gear, this problem increases the risk of damage to the vehicle's structure.

One solution could be the usage of recovery systems such as [13]. In this solution, the aircraft would have integrated a hook in its structure to take a tense or elastic cable. However, sometimes these kinds of devices are not convenient for aerial vehicles. Another approach consists of support to the aerial vehicle for landing on a ground vehicle. In this case, the challenge will be to develop a rendezvous synchronization of both vehicles.

Research projects working on cooperative control or rendezvous guidance control are focused on keeping a distance or reach to the target position such as in a refueling mission. In [14], the authors propose a guidance control strategy to align two aerial vehicles. A tanker aircraft and a receptor aircraft are controlled to maintain constraints of speed to avoid collisions. Similarly, a ground vehicle was used as mobile refueling unit, the aircraft is guided to a defined altitude with the same speed as the ground vehicle [15].

In [16], the authors proposed a cooperative control to land a fixed-wing vehicle on a ground vehicle. The aircraft descends its altitude, and the landing is carried out once both vehicles reach the same speed and position. The project evolution was reflected in [17], where the authors proposed a Model Predictive Control (MPC) for landing the aerial vehicle in a finite time on the ground vehicle. However, it becomes a complex process for the control strategy.

¹ Université de technologie de Compiègne, CNRS, Heudiasyc (Heuristics and Diagnosis of Complex Systems), CS 60319 - 60203 Compiègne Cedex, France. (aalatorr, pcastillo, rlozano)@hds.utc.fr

² Center of Research and Advanced Studies of the National Polytechnic Institute (CINVESTAV). armando.alatorre@cinvestav.mx

In this work, we propose a cooperative control strategy for landing a fixed-wing vehicle on a moving ground vehicle. The control strategy consists of guiding the fixed-wing drone following a hyperbolic trajectory. The desired trajectory is designed to perform a soft descending flight until reaches the ground vehicle's altitude. At the same time, the ground vehicle needs to control its speed and direction to reach the fixed-wing drone's position to receive it for landing. The closed-loop stability of both systems has been determined using the Lyapunov theory.

The manuscript is organized as follows: mathematical preliminaries are presented in Section II. The problem statement is given in Section III. The landing control strategy composed by the controllers of the fixed-wing vehicle and ground vehicle is described in Section IV. Main graphs from simulation results when validating the proposed strategy are shown in Section V. Section VI presents the concluding remarks and future research directions.

II. MATHEMATICAL PRELIMINARIES

The nonlinear motion equations for a fixed wing drone described in [18] can be written as

$$\begin{aligned} \dot{x} = & (\cos \theta \cos \psi) u + (\sin \phi \sin \theta \cos \psi - \cos \phi \sin \psi) v \\ & + (\cos \phi \sin \theta \cos \psi + \sin \phi \sin \psi) w \end{aligned} \quad (1)$$

$$\begin{aligned} \dot{y} = & (\cos \theta \sin \psi) u + (\sin \phi \sin \theta \sin \psi + \cos \phi \cos \psi) v \\ & + (\cos \phi \sin \theta \sin \psi - \sin \phi \cos \psi) w \end{aligned} \quad (2)$$

$$\dot{z} = u \sin \theta - (\sin \phi \cos \theta) v + (\cos \phi \cos \theta) w, \quad (3)$$

$$\dot{u} = rv - qw - g \sin \theta + \frac{A_u}{m} + \frac{\rho S_h C_h}{2m} [(k_r \delta_t)^2 - V_a^2], \quad (4)$$

$$\dot{v} = pw - ru + g \sin \phi \cos \theta + \frac{A_v}{m}, \quad (5)$$

$$\dot{w} = qu - pu + g \cos \theta \cos \phi + \frac{A_w}{m}, \quad (6)$$

$$\dot{\phi} = p + q \sin \phi \tan \theta + r \cos \phi \tan \theta \quad (7)$$

$$\dot{\theta} = q \cos \phi - r \sin \theta, \quad (8)$$

$$\dot{\psi} = q \sin \phi \sec \theta + r \cos \phi \sec \theta \quad (9)$$

$$\dot{p} = \Gamma_1 pq - \Gamma_2 qr + \tau_p \quad (10)$$

$$\dot{q} = \Gamma_5 pr - \Gamma_6 (p^2 + r^2) + \frac{1}{J_y} \tau_q \quad (11)$$

$$\dot{r} = \Gamma_7 pq - \Gamma_1 qr + \tau_r. \quad (12)$$

where (x, y, z) represent the position in the inertial frame $\{I\}$, the linear velocities (u, v, w) are described in the body frame $\{B\}$. The Euler angles are described as: ϕ for the roll angle, θ for the pitch angle, and ψ for the yaw angle. (p, q, r) describe the rotational rates in the body frame. The vehicle's mass is given by m , and terms related to the inertia moments are denoted by $\Gamma_{(\cdot)}$.

The air density is denoted as ρ , the coefficient of motor efficiency is represented by k_r , the airspeed is defined as V_a , the area and the aerodynamic coefficient of the propeller are represented by S_h and C_h , respectively.

In addition, (A_u, A_v, A_w) represent the aerodynamic forces, which are described as

$$\begin{bmatrix} A_u \\ A_v \\ A_w \end{bmatrix} = \frac{\rho V_a^2 S_a}{2} \begin{bmatrix} C_x(\alpha) + C_{xq}(\alpha) \frac{c_a q}{2V_a} + C_{x\delta_e}(\alpha) \delta_e \\ C_{y0} + C_{y\beta} \beta + \frac{C_{yp} b p}{2V_a} + \frac{C_{yr} b r}{2V_a} + C_{y\delta_a} \delta_a + C_{y\delta_r} \delta_r \\ C_z(\alpha) + C_{zq}(\alpha) \frac{c_a q}{2V_a} + C_{z\delta_e}(\alpha) \delta_e \end{bmatrix} \quad (13)$$

where the surface area of the wing is denoted as S_a , the mean chord of the wing is represented as c_a , and the wingspan is given by b . The control inputs for an airplane with classical configuration are given by the engine input δ_t , the elevator deflection δ_e , the ailerons δ_a , and the rudder δ_r .

The aerodynamics forces coefficients for the longitudinal subsystems, C_x and C_z , depend on the angle of attack α , the pitch angular rate q , and elevator deflection δ_e .

The lateral coefficients are in function of the side-slip angle β , roll and yaw angular rates (p and r), the ailerons δ_a and rudder δ_r control inputs.

The moments related to rotational rates are described as

$$\begin{bmatrix} \tau_p \\ \tau_q \\ \tau_r \end{bmatrix} = \begin{bmatrix} \frac{\rho V_a^2 S_a b}{2} C_p \\ \frac{\rho V_a^2 S_a c_a}{2} C_m \\ \frac{\rho V_a^2 S_a b}{2} C_r \end{bmatrix} \quad (14)$$

where

$$\begin{bmatrix} C_p \\ C_m \\ C_r \end{bmatrix} = \begin{bmatrix} C_{p0} + C_{p\beta} \beta + C_{pp} \frac{bp}{2V_a} + C_{pr} \frac{br}{2V_a} + C_{p\delta_a} \delta_a + C_{p\delta_r} \delta_r \\ C_m(\alpha) + C_{mq} \frac{c_a q}{2V_a} + C_{m\delta_e} \delta_e \\ C_{r0} + C_{r\beta} \beta + C_{rp} \frac{bp}{2V_a} + C_{rr} \frac{br}{2V_a} + C_{r\delta_a} \delta_a + C_{r\delta_r} \delta_r \end{bmatrix} \quad (15)$$

The aerodynamic coefficients (13) and (15), and inertia terms (10)-(12) are described with more details in [18].

Finally, the airspeed, the angle of attack, and the side-slip angle can be denoted with the form:

$$V_a = \sqrt{u^2 + v^2 + w^2} \quad (16)$$

$$\alpha = \operatorname{atan} \left(\frac{w}{u} \right) \quad (17)$$

$$\beta = \operatorname{asin} \left(\frac{v}{V_a} \right) \quad (18)$$

In this work, we will use also a ground vehicle (GV), hence, its mathematical motion equations can be described as in [19]:

$$\dot{x}_g = V_g \cos \psi_g \quad (19)$$

$$\dot{y}_g = V_g \sin \psi_g \quad (20)$$

$$\dot{\psi}_g = \frac{V_g}{l_f} \tan u_s \quad (21)$$

$$\dot{V}_g = u_t \quad (22)$$

where (x_g, y_g) represent the ground vehicle's positions, ψ_g denotes its respectively yaw angle. The speed of the ground vehicle is defined by V_g , the distance from the wheels to the mass center of the vehicle defines as l_f . The steering control input is denoted as u_s and the throttle input is represented by u_t . Finally, the altitude of the vehicle is defined as z_g .

III. PROBLEM STATEMENT

Landing stage is a critical maneuver for fixed-wing drones imply a high number of accidents caused by the pilots' inexperience or crosswind disturbances. For solving this problem, some solutions have been proposed such as recovery systems, which are popular for creative maneuvers to capture aerial vehicles. However, most of these techniques are considered as aggressive maneuvers since the capture form or braking the aircraft increases the risk of damaging its structure.

Our solution is based on a cooperative control strategy for landing a fixed-wing drone on a moving ground vehicle, see Figure 1. Both vehicles are navigating in autonomous mode exchanging information to carry out the landing challenge.

The control strategy for the fixed-wing vehicle is will be to perform an alignment stage in order to navigate straight thorough the mission. After that, the aerial vehicle will execute a trajectory tracking to perform a descending flight until reaches the ground vehicle's altitude.

Otherwise, the ground vehicle will have the task of following and aligning itself to the aircraft's position. Thus, a control algorithm will be developed to orient the ground vehicle to the direction of the aircraft using the steering control. Besides, the ground vehicle's speed will be also controlled to reach the aircraft's speed.

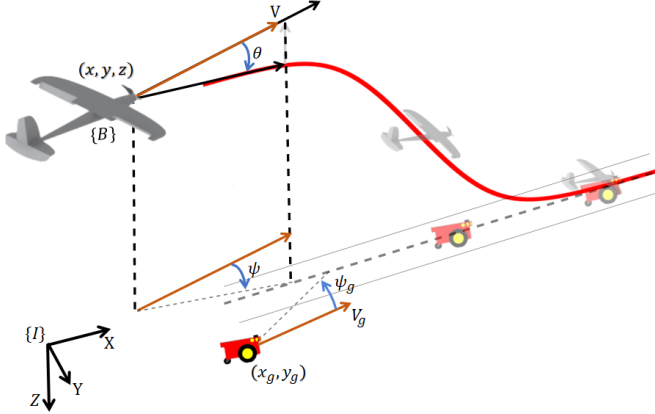


Fig. 1: Representation of the control strategy for landing a fixed-wing drone on a moving ground vehicle.

A. Desired trajectory

The desired trajectory is proposed to perform a descending flight. The trajectory is based on a hyperbolic tangent function, which depends on the time t .

The desired trajectory is defined as follows

$$z_d = \frac{h_D}{2} - \frac{h_D}{2} \tanh\left(\frac{t - t_m}{\mu}\right) + z_g \quad (23)$$

where h_D represents the distance between initial reference altitude h_T and the ground vehicle's altitude z_g . The time t_m is related to the mean altitude of the trajectory, and μ modifies the inclination of the altitude descending.

The desired trajectory is designed to reach the altitude of the ground vehicle, see Figure 2. Therefore, the landing is carried out since the ground vehicle is autonomous controlled to maintain its position with respect to the aircraft position in the x - y plane.

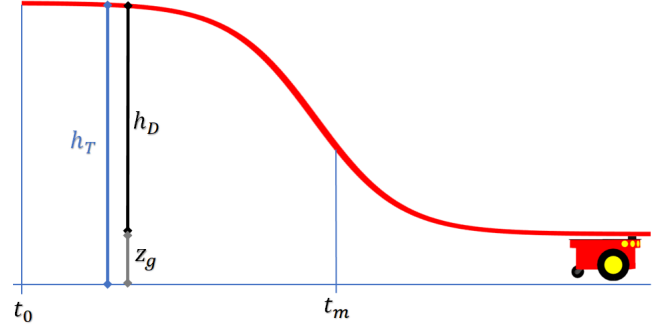


Fig. 2: Study of the parameters of the desired trajectory.

IV. LANDING CONTROL STRATEGY

Our control methodology for landing a fixed-wing drone on a moving ground vehicle contains the control designs of both vehicles. For the aerial vehicle, its lateral subsystem is controlled to be aligned towards a direction in the longitudinal plane (x, z) . These lateral motions will not be aggressive maneuvers, i.e., the aircraft will execute slow displacement reaching small angles. The last stage for the aerial vehicle, will be a tracking control algorithm, which is proposed to perform a descending flight reaching the ground vehicle's altitude. The control strategy for the ground vehicle will be designed to track the aerial vehicle's position, so that, the ground vehicle aligns and controls its speed relative to the drone.

A. Fixed-wing vehicle controllers

1) *Side-slip angle stabilization*: The aircraft alignment with respect to the airspeed vector is carried out stabilizing the side-slip angle. Using the Lyapunov stability analysis, we propose a positive function as $V_1 = \frac{1}{2}\beta^2$. Then, differentiating the previous function and using (18), it yields

$$\dot{V}_1 = \left(\frac{pw - ru + g \sin \phi \cos \theta + \frac{\rho V_a^2 S_a}{2m} C_Y}{V_a \cos \beta} \right) e_\beta < 0 \quad (24)$$

Therefore for making $\beta \rightarrow 0$, we propose the rudder control input δ_r as

$$\delta_r = \frac{-\left(C_{lat_Y} + \left[C_{Y_0} + C_{Y_p} \frac{bp}{2V_a} + C_{Y_r} \frac{br}{2V_a} + C_{Y_{\delta_a}} \delta_a\right]\right)}{C_{Y_{\delta_r}}} \quad (25)$$

where $C_{lat_Y} = \frac{2m}{\rho V_a^2 S_a} [pw - ru + g \cos \theta \sin \phi] + k_1 e_\beta$, with $k_1 > 0$.

2) *Lateral alignment*: Notice that firstly, the aircraft focuses on aligning with the y-axis, maintaining straight throughout the descending flight. Thus, considering small angles for the aircraft lateral maneuvers, we can express the lateral dynamic related to the y-axis as follows

$$\dot{y} = \psi(u \cos \theta + v \phi \sin \theta + w \sin \theta) - w \phi \quad (26)$$

Defining y_d as a constant desired position, we can express that $e_y = y - y_d$. Then, proposing a positive function as $V_2 = \frac{1}{2}e_y^2$, it follows that

$$\begin{aligned} \dot{V}_2 &= e_y \dot{e}_y \\ &= e_y [\psi(u \cos \theta + v \phi \sin \theta + w \sin \theta) - w \phi] \end{aligned} \quad (27)$$

Expressing the desired yaw angle as

$$\psi_d = \frac{w \phi - k_2 e_y}{u \cos \theta + v \phi \sin \theta + w \sin \theta} \quad (28)$$

where $k_2 > 0$, implies that if $\psi \rightarrow \psi_d$ then $e_y \rightarrow 0$ and $y \rightarrow y_d$.

Using the Lyapunov stability analysis for the yaw error, which is given by $e_\psi = \psi - \psi_d$, a positive function is proposed as $V_3 = \frac{1}{2}e_\psi^2$, such that its differentiation must satisfy the Lyapunov condition $\dot{V}_3 = \dot{e}_\psi e_\psi < 0$. Analyzing the previous equation it follows that

$$(q\phi + r)e_\psi < 0, \quad (29)$$

Considering the above equation, the desired roll angle ϕ_d can be described as

$$\phi_d = \frac{-r - e_\psi}{q}. \quad (30)$$

From (10), the aileron control input can be proposed as

$$\delta_a = \frac{-C_{latP} - \left[C_{p0} + C_{pp} \frac{bp}{2V_a} + C_{pr} \frac{br}{2V_a} + C_{p\delta_r} \delta_r \right] - \eta_\phi}{C_{p\delta_a}}, \quad (31)$$

where

$$C_{latP} = \frac{2}{\rho V_a^2 S_a b} (\Gamma_1 pq - \Gamma_2 qr). \quad (32)$$

Notice that equation (31) involves the dynamic behavior

$$\eta_\phi = k_{p\phi}(\phi - \phi_d) + k_{d\phi}\dot{\phi}, \quad (33)$$

where, $k_{p\phi}$ and $k_{d\phi}$ are the proportional and derivative gains, respectively.

3) *Airspeed control*: From the airspeed expression in (16), it is possible to determine its derivative based on the rotation from wind frame to the body frame as follows

$$\dot{V}_a = \dot{u} \cos \alpha + \dot{w} \sin \alpha \quad (34)$$

using again the Lyapunov analysis, and defining the airspeed error as $e_{V_a} = V_a - V_{a,d}$. We can propose a positive function as $V_4 = \frac{1}{2}e_{V_a}^2$. It implies that

$$\dot{V}_4 = e_{V_a} \left(\dot{u} \cos \alpha + \dot{w} \sin \alpha - \dot{V}_{a,d} \right) \quad (35)$$

Introducing (4) into the above equation, the engine control input can be determined as

$$\begin{aligned} \delta_t^2 &= \frac{V_a^2}{k_r^2} \left(\frac{1}{\cos \alpha} - \frac{S_a}{S_h C_h} A_u \right) \\ &+ \frac{2m}{\rho S_h C_h k_r^2} \left(qw + g \sin \theta + \frac{\dot{V}_{a,d} - e_{V_a}}{\cos \theta} - \frac{\dot{w} \tan \alpha}{2m} \right) \end{aligned} \quad (36)$$

Therefore, $\dot{V}_4 = -e_{V_a}^2 < 0$. Then, it follows that $V_a \rightarrow V_{a,d}$, implying that $\dot{w} \rightarrow 0$ and $\dot{u} \rightarrow 0$.

4) *Altitude stabilization*: The altitude analysis is focused on the Lyapunov theory with the goal to determine a desired pitch angle, which will guarantee altitude stabilization. Therefore, an elevator control input is designed to modify the pitch angle of the aircraft.

Defining a desired altitude z_d , the altitude error can be expressed as $e_z = z - z_d$. Thus, a positive function is proposed as $V_5 = \frac{1}{2}e_z^2$, which must satisfy the Lyapunov stability properties, $V_5 > 0$ and $\dot{V}_5 < 0$.

Differentiating V_5 , it yields that $\dot{V}_5 = e_z \dot{e}_z < 0$. Once the lateral dynamics are stabilized, then the longitudinal equations can be simplified. Thus, we can rewrite V_5 using \dot{z} from (3),

$$\dot{V}_5 = e_z(u \sin \theta - w \cos \theta - \dot{z}_d) < 0. \quad (37)$$

Observe that, (37) can be simplified dividing the expression by $\cos \theta$,

$$\frac{\dot{V}_5}{\cos \theta} = e_z(u \tan \theta - w - \frac{\dot{z}_d}{\cos \theta}) < 0. \quad (38)$$

The previous is satisfied for $-\frac{\pi}{2} < \theta < \frac{\pi}{2}$. Therefore, using (38) for defining θ_d , it follows

$$\theta_d = \tan^{-1} \left(\frac{w + \frac{\dot{z}_d}{\cos \theta} - e_z}{u} \right). \quad (39)$$

Substituting (39) into (38), we will obtain that $-e_z^2 < 0$. Then, the goal will be to propose a controller such that $\theta \rightarrow \theta_d$, this will imply that $e_z \rightarrow 0$ and then $z \rightarrow z_d$.

Computing the first and second derivative of the equation (39), it yields

$$\dot{\theta}_d = \frac{u \left(\frac{\ddot{z}_d \cos \theta + \dot{z}_d \dot{\theta} \sin \theta}{\cos^2 \theta} - \dot{e}_z \right)}{u^2 + \left(w + \frac{\dot{z}_d}{\cos \theta} - e_z \right)^2} \quad (40)$$

$$\begin{aligned} \ddot{\theta}_d &= \frac{u(-\ddot{e}_z + \cos^2 \theta \varrho_1)}{u^2 + \left(w + \frac{\dot{z}_d}{\cos \theta} - e_z \right)^2} + \frac{u(2\dot{\theta}^2 \cos \theta \sin^2 \theta)}{u^2 + \left(w + \frac{\dot{z}_d}{\cos \theta} - e_z \right)^2} \\ &- \frac{2u \left(w + \frac{\dot{z}_d}{\cos \theta} - e_z \right) \left(\frac{\ddot{z}_d \cos \theta + \dot{z}_d \dot{\theta} \sin \theta}{\cos^2 \theta} - e_z \right)^2}{\left(u^2 + \left(w + \frac{\dot{z}_d}{\cos \theta} - e_z \right)^2 \right)^2} \end{aligned} \quad (41)$$

where

$$\varrho_1 = \ddot{z}_d(\cos \theta + \dot{\theta} \sin \theta) + \dot{z}_d(\dot{\theta}^2 \cos \theta + \ddot{\theta} \sin \theta + \ddot{\theta} \sin \theta) \quad (42)$$

5) *Pitch control*: A tracking controller is designed to modify the pitch angle using the elevator control input based on the feedback state approach.

The pitch dynamics can be described as

$$\dot{\theta} = q \quad (43)$$

$$\dot{q} = \frac{\rho V_a^2 S c}{2J_y} C_m. \quad (44)$$

The pitch error can be expressed as $e_\theta = \theta - \theta_d$. Then, proposing the following positive function

$$V_6 = \frac{1}{2}(\theta - \theta_d)^2 \quad (45)$$

It implies that

$$\begin{aligned} \dot{V}_6 &= (\theta - \theta_d) \left[\dot{e}_\theta + (\ddot{\theta} - \ddot{\theta}_d) \right] \\ &= (\theta - \theta_d) \left[\dot{e}_\theta - \ddot{\theta}_d + \frac{\rho V_a^2 S_a c_a}{2J_y} C_m \right] \end{aligned} \quad (46)$$

Therefore, the pitch dynamics can be stabilized using the following controller

$$\begin{aligned} \delta_e &= \frac{1}{C_{m_{\delta_e}}} \left[- \left(C_{m_0} + C_{m_\alpha} \alpha + C_{m_q} \frac{c_a}{2V_a} q \right) \right. \\ &\quad \left. + \frac{2J_y}{\rho V_a^2 S_a c_a} \left(-\dot{e}_\theta + \ddot{\theta}_d - \frac{1}{2}(\theta - \theta_d) \right) \right], \end{aligned} \quad (47)$$

where k_{θ_p} and k_{θ_d} are positive gains. Substituting (47) into (46), yields

$$\dot{V}_6 = -V_6 < 0 \quad (48)$$

Notice that $e_\theta \rightarrow 0$ and $\dot{e}_\theta \rightarrow 0$, that is, $\theta \rightarrow \theta_d$ and $\dot{\theta} \rightarrow \dot{\theta}_d$. Therefore, it implies that $q \rightarrow 0$, $e_z \rightarrow 0$, and $\dot{z} \rightarrow 0$.

B. Ground vehicle controllers

The goal of the control design for the ground vehicle is to track the position of the fixed-wing drone in the $x - y$ plane. First, we present the throttle control input u_t in order to stabilize the speed of the ground vehicle with respect to the drone's airspeed. Then, the steering control input u_s is developed to align the ground vehicle to the aircraft.

1) *Throttle controller*: Considering the error between the aircraft and ground vehicle positions in the x -axis, then the following expression can be written

$$e_{\zeta_x} = x - x_g \quad (49)$$

$$\dot{e}_{\zeta_x} = \dot{x} - \dot{x}_g \quad (50)$$

$$\ddot{e}_{\zeta_x} = \ddot{x} - \ddot{x}_g \quad (51)$$

where

$$\ddot{x}_g = \dot{V}_g \cos \psi_g + V_g \dot{\psi}_g \sin \psi_g \quad (52)$$

Now, the Lyapunov analysis will be carried out considering the following positive function

$$V_7 = \frac{1}{2} (e_{\zeta_x} + \dot{e}_{\zeta_x})^2 = \frac{1}{2} \vartheta_x^2 \quad (53)$$

Differentiating the previous equation, it yields

$$\dot{V}_7 = \vartheta_x \left(\dot{e}_{\zeta_x} + \ddot{x} - \dot{V}_g \cos \psi_g + V_g \dot{\psi}_g \sin \psi_g \right) \quad (54)$$

We propose a feedback state controller as

$$u_t = \frac{1}{\cos \psi_g} \left(V_g \dot{\psi}_g \sin \psi_g + \ddot{x} + \dot{e}_{\zeta_x} + \frac{1}{2} k_3 \vartheta_x \right) \quad (55)$$

introducing (55) into (54), it yields

$$\dot{V}_7 = -k_3 V_7 \quad (56)$$

Therefore, $e_{\zeta_x} \rightarrow 0$ and $\dot{e}_{\zeta_x} \rightarrow 0$, that is, $x_g \rightarrow x$ and $\dot{x}_g \rightarrow \dot{x}$.

2) *Steering controller*: Define the error related with the y -axis as $e_{\zeta_y} = y - y_g$. Then, a positive function is proposed as $V_8 = \frac{1}{2} \vartheta_y^2$, where $\vartheta_y = e_{\zeta_y} + \dot{e}_{\zeta_y}$.

Computing the derivative of the above function, it yields

$$\dot{V}_8 = \vartheta_y \left(\dot{e}_{\zeta_y} + \ddot{y} - \dot{V}_g \sin \psi_g - \frac{V_g^2}{l_f} \cos \psi_g \tan u_s \right) \quad (57)$$

Proposing the steering control input as

$$u_s = \text{atan} \left(\frac{l_f}{V_g^2 \cos \psi_g} \left[-\dot{V}_g \sin \psi_g + \ddot{y} + \dot{e}_{\zeta_y} + \frac{1}{2} k_4 \vartheta_y \right] \right) \quad (58)$$

where $k_4 > 0$, it implies that $\dot{V}_8 \leq -k_4 V_8 < 0$. Thus, $e_{\zeta_y} \rightarrow 0$ and $\dot{e}_{\zeta_y} \rightarrow 0$, that is, $y_g \rightarrow y$ and $\dot{y}_g \rightarrow \dot{y}$.

V. SIMULATION RESULTS

The landing control strategy is implemented in numerical simulations to validate the control algorithm performances in closed loop. The strategy is designed to align the aerial drone in a certain direction for performing a descending flight. Moreover, the ground vehicle is controlled to reach the reflected position of the aircraft in the x - y plane.

For simulations, the initial position of the ground vehicle is defined in $(x_g(0), y_g(0)) = (0, -2)$ in meters with $\psi_g(0) = 0.57^\circ$, and the aircraft's position is given in $(x(0), y(0), z(0)) = (-10, 2, 10)$ m with $\psi(0) = 0^\circ$. The fixed-wing drone regulates its airspeed to a constant minimum phase (6 m/s) with the goal that the ground vehicle will be able to reach the aircraft position.

The aerodynamic parameters of the aircraft are described in the Table I.

The desired trajectory's parameters are described as follows: $h_D = 9$ meters, $t_m = 16$ seconds, $\mu = 6$, $z_g = 1$ m and $l_f = 0.3$ m. The steering control input is saturated in the region $[-20^\circ, 20^\circ]$ and the motor by $[0, 3]$.

The simulation result of the landing strategy is illustrated in a 3D space in Figure 3. Notice that the aerial vehicle aligns to the x -axis. Then, the fixed-wing vehicle performs the descending flight until reach the ground vehicle position. However, the ground vehicle follows the aircraft position, which is tracking a long the mission.

In Figure 4, the performance of the fixed-wing vehicle to carry out the trajectory tracking is presented. The descending trajectory imposes the aircraft to reduces its altitude from 10 meters to 1 meter, allowing the landing on the GV's top.

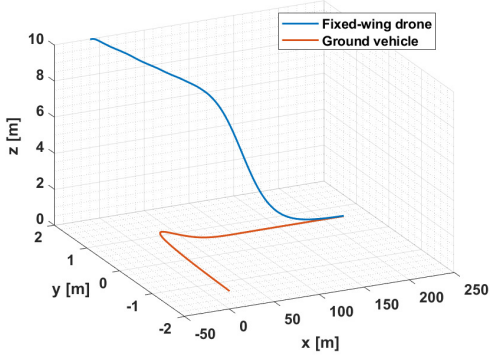


Fig. 3: Landing control strategy performance in a 3D space.

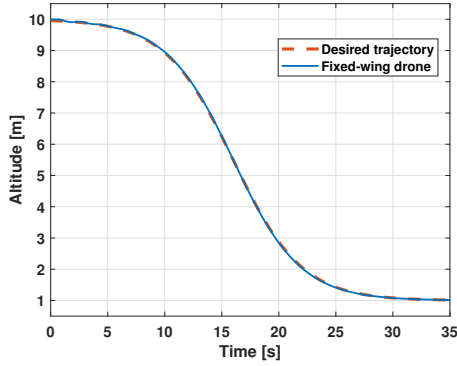


Fig. 4: Tracking results of the descending trajectory.

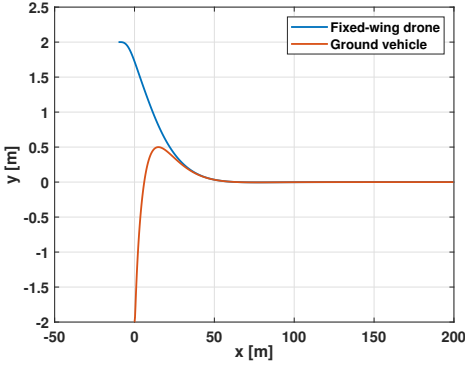


Fig. 5: Simulation result of landing strategy in the x - y plane.

In Figure 5, we present the alignment in the $x - y$ plane. Observe in this figure, the aircraft stabilizes its position to keep its reference equal to zero. Similarly, the ground vehicle aligns to the relative position of the airplane with the goal to guarantee that the ground vehicle catches the drone.

As previously mentioned, the aircraft regulates its airspeed to a constant minimum value. Therefore, the ground vehicle increases its speed to be able of reaching the aircraft position. The speed performance of the ground vehicle to reach 6 m/s, i.e., the aircraft's airspeed can be observed in Figure 6. In Figure 7, we can analyze the convergence of the ground vehicle to the drone's position in the x and y axes. The speed error is presented in Figure 8. Notice from this figure that speed error required to align the ground vehicle is minimum.

Parameters	Value	Parameters	Value
C_{L_0}	0.4029	C_{D_0}	0.0256
C_{L_α}	4.64	C_{D_α}	0.1749
C_{L_q}	7.4431	C_{D_q}	0
$C_{L_{\delta_e}}$	-0.42108	$C_{D_{\delta_e}}$	0.00528
C_{m_0}	-0.0408	C_{m_α}	-1.0454
C_{m_q}	-8.9585	$C_{m_{\delta_e}}$	-1.09407
S_h	0.0314	C_h	1
K_r	8	C_{D_p}	0.027
m	0.824	J_y	0.02453
AR	6.54	c_a	0.168
M	50	α_0	0.4712
S_a	0.185	b	1.1
$C_{y_0}=C_{l_0}=C_{l_r}$	0	$C_{n_0}=C_{n_{\delta_a}}=C_{n_{\delta_r}}$	0
C_{y_b}	-0.16451	C_{n_β}	0.058246
C_{y_p}	-0.12525	C_{n_p}	-0.016292
C_{y_r}	0.13822	C_{n_r}	-0.046933
$C_{y_{\delta_a}}$	0.04111	J_x	0.02628
$C_{y_{\delta_r}}$	0.09977	J_z	0.04811
C_{l_β}	-0.054443	J_{xz}	-0.0009316
C_{l_p}	-0.48364	$C_{l_{\delta_a}}$	0.0287
C_{l_r}	0.069133	-	-

TABLE I: Aerodynamic parameters of the reference aircraft.

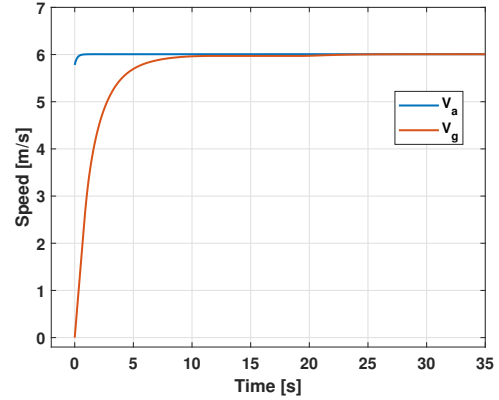


Fig. 6: Regulation performance of the speed of both vehicles.

Besides, the aircraft presents a minimum airspeed change in the descending period but the control law compensates quickly the speed. The behavior of the control input signals for the ground vehicle are presented in Figure 9.

Observe that the control inputs start the mission with a value of saturation maximum ($u_s = 20^\circ$ and $u_t = 3[N]$), and then the system is stabilized when u_s and u_t tends to 0.

In Figure 10, the performance of the longitudinal control inputs in order to evaluate the behavior during the descending flight is presented, the lateral controllers were not considered because their signals are almost zero. Thus, analyzing the elevator deflection in this figure, notice that it is almost at its limit to generate more lift because the airplane is maintaining a minimum airspeed. In addition, the behavior of the motor input tends to reduce its value in the descending flight, taking advantage of the gravity force.

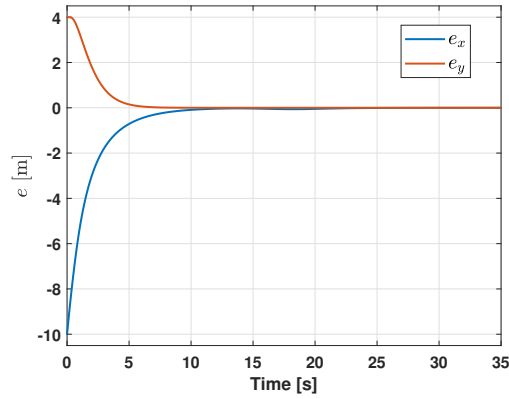


Fig. 7: Positions errors between both vehicles.

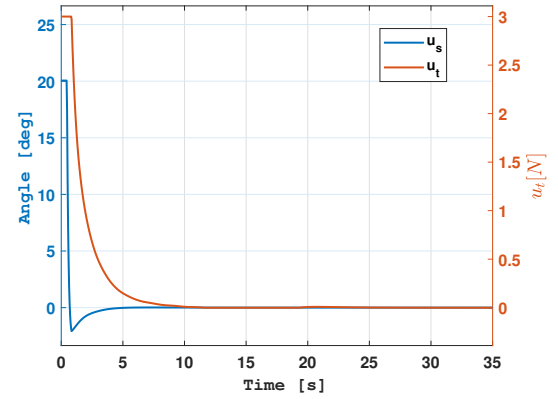


Fig. 9: Performance of u_s and u_t control inputs.

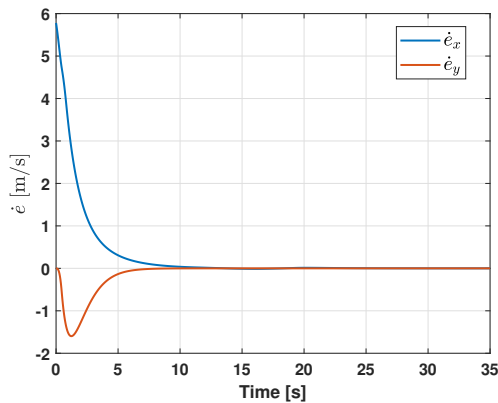


Fig. 8: Speed tracking error.

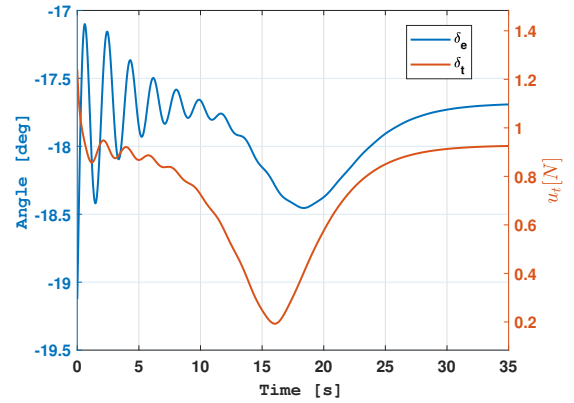


Fig. 10: Behavior of the elevator and engine control inputs.

VI. CONCLUSIONS

In this paper, an autonomous control strategy for landing a fixed-wing drone on a moving ground vehicle was presented. The strategy focused on lead the problem to a simple solution where simple tasks were assigned to each vehicle allows the rendezvous of both vehicle to guarantee a safe landing. The control strategy for the fixed-wing drone was based on the trajectory tracking for a descending flight. The desired trajectory was designed to carry out a soft descending, steering the aircraft to reach the ground vehicle's altitude. In addition, the ground vehicle executes the task of tracking the aircraft position, i.e., it aligned and regulated its speed to maintain the same position in earth plane. The controllers were designed using the Lyapunov theory.

The simulation results allowed the validation of our proposal obtaining a satisfactory result for a safe landing.

A. Future work

The main goals for future work are to improve the control designs to compensate external disturbances and system uncertainties. Moreover, the experimental validation will be carried out to lead with more realistic conditions.

ACKNOWLEDGMENT

This paper was supported by the RPV project - UTC foundation and the Mexican National Council of Science and Technology - CONACyT.

REFERENCES

- [1] Š. Čerba, J. Lúley, B. Vrban, F. Osuský, & V. Nečas. "Unmanned radiation-monitoring system". IEEE Transactions on Nuclear Science, 67(4), 636-643, 2020.
- [2] Barber, D. B., Redding, J. D., McLain, T. W., Beard, R. W., & Taylor, C. N. (2006). Vision-based target geo-location using a fixed-wing miniature air vehicle. Journal of Intelligent and Robotic Systems, 47(4), 361-382.
- [3] T. Oliveira, & P. Encarnação. "Ground target tracking control system for unmanned aerial vehicles". Journal of Intelligent & Robotic Systems, 69, 373-387, 2013.
- [4] T. M. Cabreira, C. D. Franco, P. R. Ferreira and G. C. Buttazzo. "Energy-Aware Spiral Coverage Path Planning for UAV Photogrammetric Applications". IEEE Robotics and Automation Letters, vol. 3, no. 4, pp. 3662-3668, Oct. 2018.
- [5] P. Iscold, G. A. S. Pereira and L. A. B. Torres. "Development of a Hand-Launched Small UAV for Ground Reconnaissance". IEEE Transactions on Aerospace and Electronic Systems, vol. 46, no. 1, pp. 335-348, Jan. 2010.
- [6] Z. Qu. "Cooperative control of dynamical systems: applications to autonomous vehicles" London: Springer. (Vol. 3). 2009.
- [7] M. Varga, J. C. Zufferey, Heitz, G. H. M. Zufferey, & D. Floreano. "Evaluation of control strategies for fixed-wing drones following slow-moving ground agents". Robotics and Autonomous Systems, 72, 285-294, (2015).

- [8] T. Elijah, R. S. Jamisola, Z. Tjiparuro, & M. Namoshe. "A review on control and maneuvering of cooperative fixed-wing drones". *International Journal of Dynamics and Control*, 9(3), 1332-1349, (2021).
- [9] Jantawong, J., & Deelertpaiboon, C. (2018, July). "Automatic landing control based on GPS for fixed-wing aircraft". In 2018 15th International Conference on Electrical Engineering/Electronics, Computer, Telecommunications and Information Technology (ECTI-CON) (pp. 313-316). IEEE.
- [10] M. Ruchanurucks, P. Rakprayoon, & S. Kongkaew. "Automatic Landing Assist System Using IMU+ P n P for Robust Positioning of Fixed-Wing UAVs". *Journal of Intelligent & Robotic Systems*, 2018, 90(1), 189-199.
- [11] O. A. Yakimenko, I. I. Kaminer, W. J. Lentz, & P. A. Ghyzel. "Unmanned aircraft navigation for shipboard landing using infrared vision". *IEEE Transactions on Aerospace and Electronic Systems*, 2002, 38(4), 1181-1200.
- [12] D. Zhang, & X. Wang. "Autonomous landing control of fixed-wing uavs: from theory to field experiment". *Journal of Intelligent & Robotic Systems*, 2017, 88(2-4), 619.
- [13] Landing A Drone Aircraft With No Runway: Unique 'SkyHook' Recovery System. [Online] <https://www.youtube.com/watch?v=J4uJ4yShEDA&t=2s>
- [14] A. Tsukerman, M. Weiss, T. Shima, D. Löbl, & F. Holzapfel. "Optimal rendezvous guidance laws with application to civil autonomous aerial refueling". *Journal of Guidance, Control, and Dynamics*. 2018; 41(5): 1167-1174.
- [15] A. Rucco, P. B. Sujit, A. P. Aguiar, J. B. De Sousa, & F. L. Pereira. "Optimal rendezvous trajectory for unmanned aerial-ground vehicles". *IEEE Transactions on Aerospace and Electronic Systems*. 2017; 54(2): 834-847.
- [16] T. Muskardin, G. Balmer, L. Persson, S. Wlach, M. Laiacker, A. Ollero & K. Kondak. "A novel landing system to increase payload capacity and operational availability of high altitude long endurance UAVs". *Journal of Intelligent & Robotic Systems*, 2017, 88(2), 597-618.
- [17] L. Persson, T. Muskardin, & B. Wahlberg. (2017, December). "Cooperative rendezvous of ground vehicle and aerial vehicle using model predictive control". *56th Annual Conference on Decision and Control (CDC)*, 2017, (pp. 2819-2824). IEEE.
- [18] R. W. Beard and T. W. McLain, "Small Unmanned Aircraft: Theory and Practice", 1st ed. Princeton, NJ: Princeton Univ. Press, 2012.
- [19] R. Rajamani, "Vehicle dynamics and control". *Springer Science & Business Media* 2011.